Low-Impedance Low-Artifact PEDOT:PSS -Coated Graphene Electrodes Towards High Density Optogenetic Electrophysiology

Jinyoung Park, Feng Sun, Yaowei Xie, Zheshun Xiong, and Guangyu Xu, Member, IEEE

Abstract—Graphene electrode arrays hold promise for in vivo optogenetic electrophysiology. In such studies, it would be ideal to enable spatial oversampling with a high-density array, which is challenging to maintain both low electrode impedance and low light-induced artifact. To this end, we present a 28-µm pitched, poly(3, 4-ethylenedioxythiophene):poly(styrene sulfonate) (PEDOT:PSS)-coated graphene electrode array, which was found to feature both low electrode impedance and low artifact in optogenetic electrophysiology. The resulting array was able to record the optogenetically stimulated signals, whose amplitudes increased with the stimulus intensity and maximized next to the responsive cell. Such PEDOT:PSS-coated graphene electrodes are suitable to ultimately form a flexible array for high density optogenetic electrophysiology in vivo.

Index Terms—optogenetic electrophysiology, graphene electrode array, PEDOT:PSS coating.

I. INTRODUCTION

Graphene electrode arrays [1]–[4] hold promise for *in vivo* optogenetic electrophysiology, a cell biology approach featuring high precision and cell-type specificity [5], [6]. These electrode arrays can be highly compliant, and suitable for low noise recording of cell activity with low light-induced artifact under optogenetic stimulus [1], [4], [7]. Such studies would benefit from spatial oversampling of cell network with high density arrays, which can ultimately register recorded data to individual cells [8], [9]. It is thus essential to evaluate if a high-density graphene electrode array could maintain *both* low impedance (for high signal-to-noise ratios, SNR) *and* low artifact (for high signal-to-artifact ratios, SAR) [1], [7].

To date, electrode arrays made of monolayer and four-layer graphene have been reported to allow for low artifact optogenetic electrophysiology [7]. However, these arrays were typically built in a 300-900 µm pitch [1], [2], [4], which lacks the spatial resolution needed for spatial oversampling as reported in closely packed silicon-substrated electrodes [8]. To achieve high-density optogenetic electrophysiology, graphene electrodes need to be further engineered to feature both low impedance and low artifact [4], [7]. To this end, graphene

This work was supported by the National Science Foundation under ECCS-1835268. J. Park and F. Sun contributed equally to this work.

The authors are with the Department of Electrical and Computer Engineering, University of Massachusetts at Amherst, Amherst, MA 01003 USA (e-mail: guangyux@umass.edu).

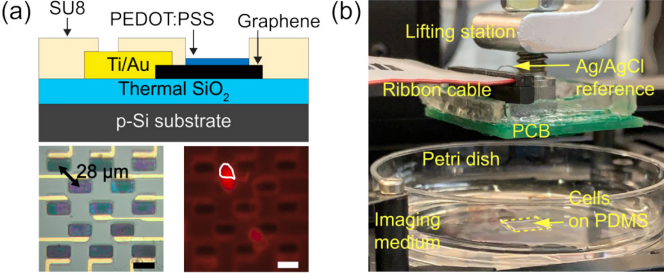


Fig. 1. Array fabrication and testing setup. (a) Schematics of a PEDOT: PSS-coated graphene electrode, a fabricated 28 μm -pitched array, and the array interfacing with cells. Scale bar, 20 μm . (b) Cell testing setup with the array packaged on a side-flipped PCB fixed on a lifting station.

electrodes coated with Pt nanoparticles [10] and poly(3, 4-ethylenedioxythiophene):poly(styrene sulfonate) (PEDOT:PSS) were recently noted for their reduced impedance [11]. Nonetheless, these surface-coated graphene electrodes have not been examined in optogenetic electrophysiology studies, which requires *both* high SNR *and* high SAR.

Here we present a 28-µm pitched PEDOT:PSS-coated graphene electrode array that features both low impedance and low artifact. Being one order denser than reported graphene arrays in optogenetic electrophysiology, our array can record optogenetically stimulated extracellular signals with SNR > 20 and SAR > 3. The signal amplitude increased with the stimulus intensity with its maximum next to the responsive cell. Such low-impedance, low-artifact electrodes are suitable to ultimately form a flexible array for high density optogenetic electrophysiology studies at the *in vivo* setting.

II. METHODS

Our array was built on chemical-vapor-deposition grown graphene wafers (ACS Material), with 3-5 layered graphene (lower sheet resistance than monolayer graphene [2]) one-time transferred to a Si/SiO₂ substrate by the standard Cu-etching method. (Fig. 1(a)). Using an O₂ based reactive-ion-etching step, we patterned graphene electrodes in a 28- μ m pitch, contacted by evaporated Ti/Au layers (no graphene damage was observed), and passivated the chip by a 4 μ m-thick SU8 layer with 21 μ m-by-10 μ m sized opening that defined the effective electrode area. We then treated the SU8 layer with an O₂-plasma step (with graphene being protected by photoresist) to enhance its hydrophilicity, which was found to improve the following electroplating [12] and cell testing steps. The array was then wire-bonded onto a printed-circuit board (PCB) and packaged by polydimethylsiloxane (PDMS) (Fig. 1(b)).

On the electrochemistry side, each electrode was configured to a three-electrode setting [4] by Gamry Reference 600+ (with a Pt wire as the counter electrode and an Ag/AgCl wire as the reference electrode) for electrochemical impedance spectroscopy (EIS) and cyclic voltammetry (CV) measurement in 1× phosphate buffer saline. We also used this three-electrode configuration to electroplate a PEDOT:PSS layer on individual electrodes. This was achieved by immersing the array in 400 µL deionized water mixed with 0.048 M PSS and 0.02 M EDOT monomer, and injecting 2.1 mA/cm² current from each graphene electrode for two consecutive 10-s periods [11].

We next cultured human embryonic kidney (HEK) 293 cells [6], [13] on a PDMS piece and co-transfected them with opsins (*ChR2*) and Ca²⁺ reporters (*jRCAMP1a*). The PDMS piece with cells facing up was later transferred to a Petri dish filled with a cell imaging medium that contained 80 mM CaCl₂, 5 mM NaCl, and 3 mM KCl (pH 7.3) as we reported before [13]. We then used an inverted fluorescence microscope (Leica) to: 1) conduct Ca²⁺ imaging with 100 ms exposure time per frame to identify optogenetically responsive cells. This was achieved by a 6.49 mW/cm² 575/22 nm excitation light pulsed at 0.5 frame per second, a 585 nm long-pass dichroic mirror, and a 632/60 nm emission filter; and 2) apply 470/40 nm optogenetic stimulus at 20.41~38.94 mW/cm² to evoke Ca²⁺ transients in cells. The 575-nm excitation light was off within the 470-nm stimulus window.

To form the array-cell contact, we side-flipped the array on the PCB and fixed it on a home-built lifting station controlled by a manual lab jack and a positioning stage. The array was then lowered, aligned to, and contacted with the responsive cells by fine-tuning the lifting station. An Ag/AgCl wire was immersed in the medium to bias it. Using an Intan RHD2164 amplifier chip synchronized with the microscope camera, we sampled extracellular signals at 10 kHz (band-pass filtered at 0.1-3 kHz); the 60 Hz noise and DC offset were removed by built-in filters of an Intan interface software.

III. RESULTS AND DISCUSSIONS

A. Electrochemical characterization

We found that the PEDOT:PSS coatting step was effective in altering the EIS and CV data of the array. After ca. 20 s of electroplating, each electrode typically dropped its EIS impedance at 1 kHz from ca. 2 M Ω to sub-100 k Ω , and increased its EIS phase in the entire frequency range (Fig. 2(a)). This result suggests that the PEDOT:PSS coating layer reduced the electrode impedance, and changed electrodes to be less capacitive [14]. At the array level, 12 out of 13 electrodes showed more than 20 times of impedance decrease (from $2.00 \pm$ $0.11 \text{ M}\Omega$ to $74 \pm 13 \text{ k}\Omega$), with one electrode (#1) showing only 3.5 times of decrease (from 2.16 M Ω to 0.60 M Ω) where the graphene flake may be degraded during electroplating (Fig. 2(b)). These sub-100 k Ω electrodes placed in a 28 μ m pitch are desired for high SNR in high-density electrophysiology [15]. Moreover, the PEDOT:PSS layer increased the current in CV curves by ca. one order. This increase is likely because the thickness of the PEDOT:PSS layer increased the effective surface area of the electrode, and thus lowered the electrode impedance with a lower charge transfer resistance and a larger double-layer capacitance [16]-[21].

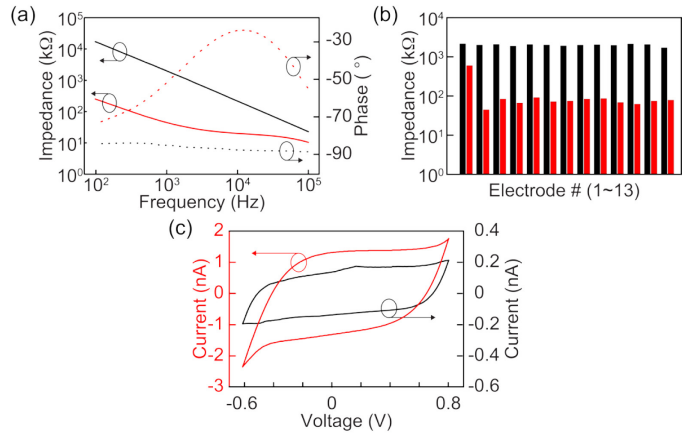


Fig. 2. Electrochemical characterization before (black) and after PEDOT: PSS coating (red). (a) EIS impedance (solid line) and phase (dashed line) of a typical electrode, (b) EIS impedance at 1 kHz of all 13 electrodes, and (c) CV of a typical electrode measured in the 10th cycle and scanned at 1000 mV/s.

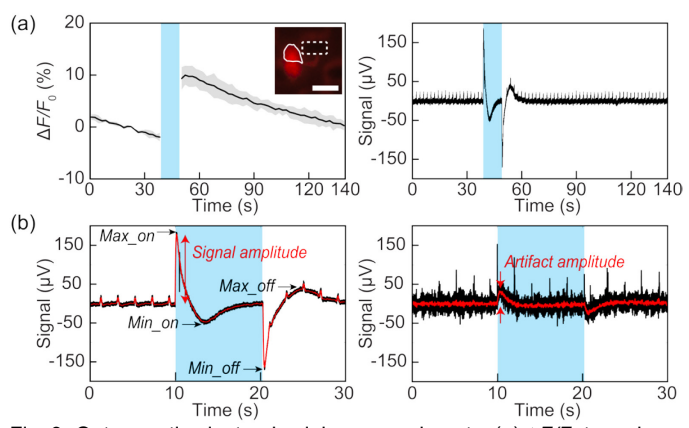


Fig. 3. Optogenetic electrophysiology experiments. (a) $\Delta F/F_0$ trace in an optogenetically responsive cell with 10-s 470-nm stimulus at 30 mW/cm² (left), and the recorded trace from its adjacent electrode (right). Shaded areas represent ± 1 SD. The inset shows the <code>jRCAMP1a</code> image of cells overlaid on the array image. Scale bar, 20 µm. (b) 30-s recording traces of the cell signal (left) and the artifact (right) in one electrode (raw data in black; 500-point adjacent-averaging data in red). All data are 3-period averaged; blue windows mark the period of 470-nm stimulus.

B. Optogenetic electrophysiology experiments

After forming the array-cell contact, we simulataneously conducted optogenetic electrophysiology and Ca^{2+} imaging, the latter serving to reaffirm optogenetic responsiveness of the targeted cell during the experiment. Here we alternately applied pulsed excitation light (to alleviate the photobleaching effect [22]) and 10-s 470/40 nm optogenetic stimulus in three consecutive 140-s periods for statistics. In each period, the F_0 value is defined as the 40-s average before the stimulus (subtracted by the background defined in [13]). The resulting positive $\Delta F/F_0$ values after stimulation (~ 9.33%) suggest an increase of intracellular Ca^{2+} level due to the optogenetically triggered Ca^{2+} flux into the responsive cell (Fig. 3(a), left).

At the same time, we found that the voltage signal recorded by the electrode next to the responsive cell showed enhanced oscillation at *both* the start *and* the end of the 470-nm stimulus (Fig. 3(a), right). Importantly, the ratio of the signal amplitude measured with cells to the artifact amplitude meaured without cells on the same electrode (*i.e.* SAR) was over 3 (from 500

-point adjacent averaging data in Fig. 3(b)), showing that our electrode can detect optogenetically evoked extracellular signals with statistical significance. On the other hand, the recorded signal trace (Fig. 3(b), left) also showed a high SNR (> 20, defined in [1]) due to the low electrode impedance; the noise peaks in a period of 2 s were likely from the weak optogenetic response from cells and the light-induced artifact from the cell emission [19], [23] (see details below).

Notably, the recorded voltage signal (*i.e.* raw data measured with cells): 1) increased at the start of the stimulus with a maximum Max_on , which then settled back to the baseline with a minimum Min_on , and 2) decreased at the end of the stimulus with a minimum Min_off , which then settled back to the baseline with a maximum Max_off . Such oscillations can be attributed to optogenetically evoked cation flux across the cell membrane [24] as follows.

At the start of 470-nm stimulus, ChR2 (a non-specific cation channel) were opened to enable the flux of cations following their concentration gradient across the cell membrane [24], [25]. Such cation flux is expected to be mainly from K⁺ and Ca²⁺ ions because our cell imaging medium includes more Ca²⁺ (80 mM) and less K⁺ (3 mM) than their intracellular concerntration (sub-mM Ca²⁺, ca. 150 mM K⁺) [23], [26], [27]. Since ChR2 has a higher permeability to K⁺ ions than Ca²⁺ ions [28], it was likely that the efflux of K⁺ ions was dominant at the beginning of the stimulus, which charged the PEDOT:PSS layer and led to the voltage increase [29]. Meanwhile, the Ca²⁺ influx counterbalanced the effect of K⁺ efflux, settling the voltage back to the baseline when the equilibrium between Ca²⁺ and K⁺ flux was established. At the end of 470-nm stimulus, ChR2 channels were closed instantly [25]. In this case, K⁺ (Ca²⁺) ions near the electrode flushed into (out of) cells via native K⁺ (Ca²⁺) ion channels to recover cells back to their resting stage [26], [27], [30]. It appears again that K⁺ influx dominated Ca²⁺ efflux when the stimulus was just off, likely due to higher permeability of K⁺ ions in native K⁺ ion channels. Importantly, such enhanced oscillations were not observed in cells that were transfected with jRCAMP1a only (not shown), suggesting that the cell signal in Fig. 3 was specific to the optogenetic effect.

On the other hand, the light-induced artifact measured with no cells (Fig. 3(b)) can result from the photo-induced electron hole pairs in the PEDOT:PSS layer and the circuitry loading effect [4]. At the start of the stimulus, photo-induced electrons (minority) rapidly got recombined due to their short lifetime [20],[32]-[34]; the un-recombined photo-induced holes left on the electrode can lead to a transient positive voltage. At the end of the stimulus, the number of photo-induced holes dropped instantly; their counter ions left near the electrode may result in a transient negative voltage. In both cases, the voltage trace settled back to the baseline within seconds, likely due to the *RC* discharging in an equivalent circuit formed by the *Randles* electrode model and the input load of the amplifiers [4].

We finally quantify the recorded signals of our coated array to examine its promise for high-density optogenetic electro-physiology. Our data showed that Max_on and Min_off values from the electrode next to the responsive cell were more than $100~\mu V$ (Fig. 4(a)), and increased with the stimulus intensity, which is likely because stronger stimulus increased the amount of cation flux by opening more ChR2 channels [13], [25]. The $Max \ off$ and $Min \ on$ values were in contrast comparable to the

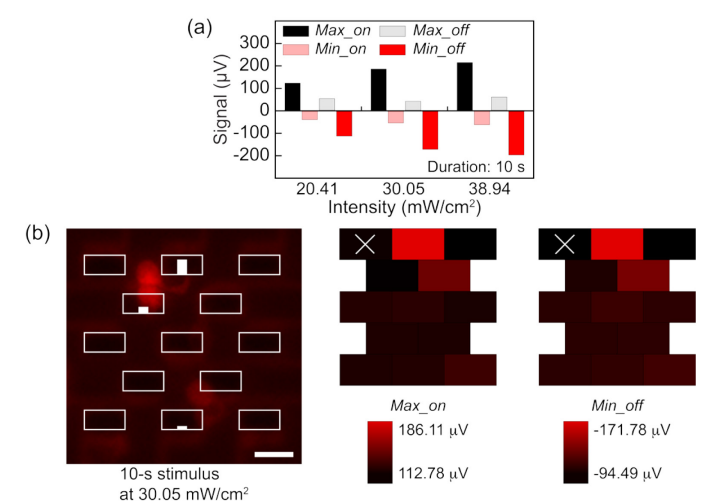


Fig. 4. Qualification of the electrophysiology data. (a) Signal amplitudes vs. 470-nm stimulus intensity. (b) $\Delta F/F_0$ mapping (white boxes indicate electrode sites) and signal amplitudes mapping (the crossed electrode failed after electroplating). The jRCAMP1a image of cells was overlaid with the array image. Bar plots show $\Delta F/F_0$ at each electrode (the height of each box is 15 %). Scale bar, 20 μ m.

measured artifact and thus not selected for analysis. Further -more, we plotted the spatial mapping of Max_on and Min_off across the array, and compared them with the $\Delta F/F_0$ values at each electrode (Fig. 4(b)). To evaluate the spatial resolution of our array, we chose a field of view with only a few sparse cells. We then normalized F_0 values according to the brightest cell, and treated the electrode regions with normalized $F_0 < 0.1$ as $\Delta F/F_0 = 0$ since these regions had no cells nearby. The electrode close to the responsive cell ($\Delta F/F_0 > 10$ %) showed maximum Max_on and Min_off values among all 12 working electrodes. This result shows our PEDOT:PSS-coated array can provide recording data that can qualitatively match the position of the optogenetically responsive cells.

IV. CONCLUSION

In sum, we presented a 28 µm-pitched PEDOT:PSS-coated graphene electrode array featuring SNR > 20 and SAR > 3 in optogenetic electrophysiology. These high density electrodes showed *both* low electrode impedance *and* low artifact, two essential features for optogenetic electrophysiology studies. The fact that SAR was over 3 in our data likely originated from the photoelectric properties of the PEDOT:PSS layer, where the charging effect from optogenetically evoked cation flux was significant compared to that from the photo-induced carriers. Such electrodes can ultimately be built on a flexible substrate (e.g. Parylene C) with integrated light sources (e.g. LEDs), which would enable high density *in vivo* optogenetic electrophysiology for a variety of cell types (e.g. neurons) [35], [36].

REFERENCES

- [1] D. Kuzum, H. Takano, E. Shim, J. C. Reed, H. Juul, A. G. Richardson, J. de Vries, H. Bink, M. A. Dichter, T. H. Lucas, D. A. Coulter, E. Cubukcu, and B. Litt, "Transparent and flexible low noise graphene electrodes for simultaneous electrophysiology and neuroimaging," *Nat. Commun.*, vol. 5, no. 5259, pp. 1-10, Oct. 2014, doi: 10.1038/ncomms6259
- [2] D.-W. Park, A. A. Schendel, S. Mikael, S. K. Brodnick, T. J. Richner, J. P. Ness, M. R. Hayat, F. Atry, S. T. Frye, R. Pashaie, S. Thongpang, Z. Ma, and J. C. Williams, "Graphene-based carbon-layered electrode array

- technology for neural imaging and optogenetic applications", *Nat. Commun.*, vol. 5, no. 5258, pp. 1-11, Oct. 2014, doi: 10.1038/ncomms6258
- [3] M. Thunemann., Y. Lu, X. Liu, K. Kılıç, M. Desjardins, M. Vandenberghe, S. Sadegh, P. A. Saisan, Q. Cheng, K. L. Weldy, H. Lyu, S. Djurovic, O. A. Andreassen, A. M. Dale, A. Devor, and D. Kuzum, "Deep 2-photon imaging and artifact-free optogenetics through transparent graphene microelectrode arrays," *Nat. Commun.*, vol. 9, no. 2035, pp. 1-12, May 2018, doi: 10.1038/s41467-018-04457-5
- [4] X. Liu, Y. Lu, E. Iseri, Y. Shi, and D. Kuzum, "A compact closed-loop optogenetics system based on artifact-free transparent graphene electrodes", Front. Neurosci., vol. 12, no.132, pp. 1-13, Mar. 2018, doi: 10.3389/fnins.2018.00132.
- [5] B. Y. Chow, X. Han, A. S. Dobry, X. Qian, A. S. Chuong, M. Li, M. A. Henninger, G. M. Belfort, Y. Lin, P. E. Monahan, E. S. Boyden, "High-performance genetically targetable optical neural silencing by light-driven proton pumps", *Nature*, vol. 463, pp. 98-102, Jan. 2010 doi: 10.1038/nature08652.
- [6] H. Zhang, E. Reichert, A. E. Cohen, "Optical electrophysiology for probing function and pharmacology of voltage-gated ion channels", *Elife*, vol. 5, no. 5:e15202, pp. 1-20, May. 2016, doi: 10.7554/eLife.15202
- [7] Y. Lu, X. Liu, and D. Kuzum, "Graphene-based neurotechnologies for advanced neural interfaces", *Curr. Opin. Biomed. Eng.*, vol. 6, pp. 138-147, Jun. 2018, doi: 10.1016/j.cobme.2018.06.001
- [8] J. Scholvin, J. P. Kinney, J. G. Bernstein, C. Moore-Kochlacs, N. Kopell, C. G. Fonstad, and E. S. Boyden, "Close-packed silicon microelectrodes for scalable spatially oversampled neural recording", *IEEE Trans. Biomed. Eng.*, vol. 63, no. 1, pp. 120-130, Feb. 2015, doi: 10.1109/TBME.2015.2406113
- [9] A. Hierlemann, U. Frey, S. Hafizovic, and F. Heer, "Growing cells atop microelectronics chips: interfacing electrogenic cells in vitro with CMOS-based microelectrode array", Proc. IEEE, vol. 99, no. 2, pp. 252-284, Oct. 2011, doi: 10.1109/JPROC.2010.2066532
- [10] Y. Lu, X. Liu, R. Hattori, C. Ren, X. Zhang, T. Komiyama, and D. Kuzum, "Ultralow impedance graphene microelectrodes with high optical transparency for simultaneous deep two-photon imaging in transgenic mice", Adv. Funct. Mater., vol. 28, no. 31, pp. 1-9, Aug. 2018, doi: 10.1002/adfm.201800002.
- [11] P. Kshirsagar, S. Dickreuter, M. Mierzejewski, C. J. Burkhardt, T. Chassé, M. Fleischer, and P. D. Jones, "Transparent graphene/PEDOT: PSS microelectrodes for electro- and optophysiology", *Adv. Mater. Tech.*, vol. 4, no. 1, pp. 1-7, Jan. 2019, doi: 10.1002/admt.201800318.
- [12] F. Walther, P. Davydovskaya, S. Zürcher, M. Kaiser, H. Herberg, A. M. Gigler, and R. W. Stark, "Stability of the hydrophilic behavior of oxygen plasma activated SU-8", *J. Micromech. Microeng.*, vol. 17, no. 3, pp. 524-531, Feb. 2007, doi: 10.1088/0960-1317/17/3/015.
- [13] D. Mao, N. Li, Z. Xiong, Y. Sun, and G. Xu, "Single-Cell Optogenetic Control of Calcium Signaling with a High-Density Micro-LED Array", iScience, vol. 21, pp. 403-412, Nov. 2019, doi: 10.1016/j.isci.2019.10.024.
- [14] A. J. Bard, L. R. Faulkner, Electrochemical Methods: Fundamentals and Applications, 2nd ed. NY, USA: Wiley, 2001, doi: 10.1023/A:1021637209564
- [15] S. F. Cogan, "Neural stimulation and recording electrodes", Annu. Rev. Biomed. Eng., vol. 10, pp. 275-309, Aug. 2008, doi: 10.1146/annurev.bioeng.10.061807.160518.
- [16] M. Ganji, A. T. Elthakeb, A. Tanaka, V. Gilja, E. Halgren, and S. A. Dayeh, "Scaling Effects on the Electrochemical Performance of poly (3, 4-ethylenedioxythiophene (PEDOT), Au, and Pt for Electrocorticography Recording," Adv. Funct. Mater., vol. 27, no. 42, pp. 1-12, Sept. 2017, doi: 10.1002/adfm.201703018
- [17] K. A. Ludwig, N. B. Langhals, M. D. Joseph, S. M. Richardson-Burns, J. L. Hendricks, and D. R. Kipke, "Poly (3, 4-ethylenedioxythiophene) (PEDOT) polymer coatings facilitate smaller neural recording electrodes," *J. Neural Eng.*, vol. 8, no. 1, pp. 1-7, Jan. 2011, doi: 10.1088/1741-2560/8/1/014001
- [18] D. Khodagholy, J. N. Gelinas, T. Thesen, W. Doyle, O. Devinsky, G. G. Malliaras, and G. Buzsáki, "NeuroGrid: recording action potentials from the surface of the brain," *Nat. Neurosci.*, vol. 18, no. 2, pp. 310-315, Feb. 2015, doi: 10.1038/nn.3905
- [19] A. Elschner, S. Kirchmeyer, W. Lovenich, U. Merker, K. Reuter, PEDOT: principles and applications of an intrinsically conductive polymer, FL, USA: CRC press, 2010, doi: 10.1201/b10318

- [20] J. Rivnay, H. Wang, L. Fenno, K. Deisseroth, and G. G. Malliaras, "Next-generation probes, particles, and proteins for neural interfacing", Sci. Adv., vol.3, no. 6, pp. 1-20, Jun. 2017. doi: 10.1126/sciadv.1601649.
- [21] S. J. Wilks, S. M. Richardson-Burns, J. L. Hendricks, D. C. Martin, and K. J. Otto, "Poly(3,4-ethylenedioxythiophene) as a Micro-Neural Interface Material for Electrostimulation," *Front. Neuroeng.*, vol. 2, no. 7, pp. 1-8, June 2009, doi: 10.3389/neuro.16.007.2009
- [22] Z. Xiong, F.-J. Hwang, F. Sun, Y. Xie, D. Mao, G.-L. Li, and G. Xu, "Spectrally filtered passive Si photodiode array for on-chip fluorescence imaging of intracellular calcium dynamics", Sci. Rep., vol. 9, no. 1, pp. 1-9, Jun. 2019, doi: 10.1038/s41598-019-45563-8
- [23] J. Y. Lin, M. Z. Lin, P. Steinbach, and R. Y. Tsien, "Characterization of engineered channelrhodopsin variants with improved properties and kinetics." *Biophys. J.*, vol. 96, no. 5, pp. 1803-1814, Mar. 2009, doi: 10.1016/j.bpj.2008.11.034
- [24] F. Zhang, J. Vierock, O. Yizhar, L. E. Fenno, S. Tsunoda, A. Kianianmomeni, M. Prigge, A. Berndt, J. Cushman, J. Polle, J. Magnuson, J. Magnuson, P. Hegemann, and K. Deisseroth, "The microbial opsin family of optogenetic tools", *Cell*, vol. 147, no. 7, pp. 1446-1457, Dec. 2011, doi: 10.1016/j.cell.2011.12.004
- [25] K. Deisseroth, and P. Hegemann, "The form and function of channelrhodopsin", *Science*, vol. 357, no. 6356, pp. 1-9, Sep. 2017, doi: 10.1126/science.aan5544
- [26] H. Lodish, A. Berk, S L. Zipursky, P. Matsudaira, D. Baltimore, J. Darnell, *Molecular Cell Biology*, 5th ed, NY, USA: W. H. Freeman, 2000.
- [27] G. Zhu, Y. Zhang, H. Xu, and C. Jiang, "Identification of endogenous outward currents in the human embryonic kidney (HEK 293) cell line", J. Neurosci. Methods, vol. 81, no. 1-2, pp. 73-81, Jun. 1998, doi: 10.1016/s0165-0270(98)00019-3
- [28] S. Kleinlogel, K. Feldbauer, R. E. Dempski, H. Fotis, P. G. Wood, C. Bamann, and E. Bamberg, "Ultralight-sensitive and fast neuronal activation with the Ca²⁺-permeable channelrhodopsin CatCh", *Nat. Neurosci.*, vol. 14, no. 4, pp. 513-518, Apr. 2011, doi: 10.1038/nn.2776
- [29] S. M. Won, E. Song, J. Zhao, J. Li, J. Rivnay, and J. A. Rogers, "Recent advances in materials, devices, and systems for neural interfaces", Adv. Mater., vol. 30, no. 30, pp. 1-19, Jul. 2018, doi: 10.1002/adma.201800534
- [30] A. Varghese, E. M. TenBroek, J. Coles. Jr., and D. C. Sigg, "Endogenous channels in HEK cells and potential roles in HCN ionic current measurements", *Prog. Biophys. Mol. Biol.*, vol. 90, no. 1-3, pp. 26-37, Jan. 2006, doi: 10.1016/j.pbiomolbio.2005.05.002
- [31] T. D.Y. Kozai, and A. L. Vazquez, "Photoelectric artefact from optogenetics and imaging on microelectrodes and bioelectronics: new challenges and opportunities", *J. Mater. Chem. B*, vol. 3, no. 25, pp. 4965-4978, Apr. 2015, doi: 10.1039/C5TB00108K
- [32] Y. Zhang, L. Chen, X. Hu, L. Zhang, and Y. Chen, "Low work-function poly (3, 4-ethylenedioxylenethiophene): Poly (styrene sulfonate) as electron-transport layer for high-efficient and stable polymer solar cells", *Sci. Rep.*, vol. 5, no. 12839, pp. 1-12, Aug. 2015, doi: 10.1038/srep12839
- [33] S. M. Sze, Physics of Semiconductor Devices, Hoboken, NJ, USA: Wiley, 1998. Doi: 10.1002/0470068329
- [34] T. V. A. G. de Oliveira, M. Gobbi, J. M. Porro, L. E. Hueso and A. M. Bittner, "Charge and spin transport in PEDOT:PSS nanoscale lateral devices;," *Nanotech.*, vol. 24, no. 47, pp. 1-10, Oct. 2013, doi: 10.1088/0957-4484/24/47/475201
- [35] J. W. Suk, A. Kitt, C. W. Magnuson, Y. Hao, S. Ahmed, J. An, A. K. Swan, B. B. Goldberg, and R. S. Ruoff, "Transfer of CVD-grown monolayer graphene onto arbitrary substrates." ACS Nano. vol. 5, no. 9, pp. 6916-6924, Sept. 2011, doi: 10.1021/nn201207c
- [36] J. W. Reddy, I. Kimukin, L. T. Stewart, Z. Ahmed, A. L. Barth, E. Towe, and M. Chamanzar, "High Density, Double-Sided, Flexible Optoelectronic Neural Probes with Embedded μLEDs," Front. Neurosci., vol.9, pp. 1-15, Aug. 2019, doi: 10.3389/fnins.2019.00745